Intelligent Switching Control of Pneumatic Cylinders by Learning Vector Quantization Neural Network

KyoungKwan Ahn*, ByungRyong Lee
School of Mechanical and Automotive Engineering, University of Ulsan, San 29, Muger2-dong, Nam-gu, Ulsan 680-749, Korea

The development of a fast, accurate, and inexpensive position-controlled pneumatic actuator that may be applied to various practical positioning applications with various external loads is described in this paper A novel modified pulse-width modulation (MPWM) valve pulsing algorithm allows on/off solenoid valves to be used in place of costly servo valves A comparison between the system response of the standard PWM technique and that of the modified PWM technique shows that the performance of the proposed technique was significantly increased A state-feedback controller with position, velocity and acceleration feedback was successfully implemented as a continuous controller A switching algorithm for control parameters using a learning vector quantization neural network (LVQNN) has newly proposed, which classifies the external load of the pneumatic actuator The effectiveness of this proposed control algorithm with smooth switching control has been demonstrated through experiments with various external loads

Key Words : Pneumatic, Switching Control, On/off Solenoid Valve, Pulse Width Modulation, Neural Network, Intelligent Control

Nomenclature

$U_{MPWM}(t)$	MPWM output
U_0	Valve opening signal
t_p	ON duty ratio of valve for one MPWM cycle
t_s	Modified duty ratio with dead-band region
t_{s1}	Modified duty ratio of on/off valve
y	Position of rodless cylinder
y_{ref}	Reference Position
ε	Maximum error limit
t_{DZ}	Dead time of valve
T	MPWM cycle time
t	Continuous time
$U(k)$	Sampled control Input of $u(t)$
U_{max}	Saturated control input for MPWM modulator
k	Discrete sequence

* Corresponding Author,
E-mail kkahn@ulsan.ac.kr
TEL +82-52-259-2282, **FAX** +82-52-259-2282
School of Mechanical and Automotive Engineering, University of Ulsan, San 29, Muger2-dong, Nam-gu, Ulsan 680-749, Korea (Manuscript **Received** June 3, 2004, **Revised** November 17, 2004)

1. Introduction

Pneumatic control systems play very important roles in industrial automation systems owing to the advantages of low cost, easy maintenance, cleanliness, ready availability and cheap power source, etc (Anderson, 1967) A particularly well-suited application for pneumatic actuators is the position control of robotic manipulators, loading/unloading systems, air balance systems and grippers, where stiff and lightweight structures are critical Unfortunately, pneumatic actuators are subject to high friction forces, dead-band due to stiction, and dead-time due to the compressibility of air These nonlinearities make accurate position control of pneumatic actuators difficult to achieve

As a result, a considerable amount of research

has been devoted to the development of various position control systems for pneumatic actuators (Noritsugu, 1995; Tang, 1995; Marchant, 1989; Kawamura, 1989). Many of these systems, though successful, use expensive proportional servo valves and pressure sensor feedback loops and the external loads are also assumed to be constant or slowly varying.

The object of this paper is to implement inexpensive on/off solenoid valves, rather than expensive servo valves, to develop a fast, accurate, inexpensive and intelligent pneumatic control system taking account of the changes of external loads. However, with solenoid valves, fine motion control is difficult to achieve because of the limitation of valve response time and its discrete on/off nature. Previous studies (Noritsugu, 1986; Noritsugu, 1987; Muto, 1993; Mishra, 1994) have tried to implement on/off solenoid valves for the position control of pneumatic actuators. Noritsugu (1995, 1996) has used the PWM method and solenoid valve to control the velocity and the position of pneumatic cylinders. Muto (1993) has used differential PWM (Pulse Width Modulation) method to control hydraulic actuators and Ahn and Tu (2004) has used intelligent switching control method in the position control of artificial muscle manipulator. These systems were successful in addressing smooth actuator motion in response to step inputs. However, some limitations still exist, such as deterioration of the performance of transient responses due to cases of abrupt changes of external loads. To overcome this problem, the MPWM (modified pulse width modulation) on/off valve control scheme and a switching control algorithm by LVQNN (Learning Vector Quantization Neural Network), have been newly proposed and control performance has been experimentally verified.

2. Pneumatic Position Control System

2.1 Experimental apparatus

A schematic diagram of the control system is shown in Fig. 1. An IBM-compatible computer (Pentium I GHz) was applied to control the on/off solenoid valve and to get experimental data. The stroke and the bore diameter of the rodless cylinder (SMC, MY1M32-1000L) were 1000 mm and 32 mm, respectively, and different masses could be attached to the table of the rodless cylinder. The displacement of the cylinder was measured by a linear scale (US Digital, resolution 0.05 mm) and the air pressure were also measured by air pressure sensor (SMC, ISE 40-01-22L) which was fed back to the computer through a 24-bit counter board (Advantech, PCL 833) and A/D board (Advantech, PCI 1731), respectively. The control signal was changed into pulse width modulated signal through our proposed MPWM algorithm. The control signal was sent to control the solid state relay and 8 pneumatic on/off solenoid valves (MAC, 111B-872JD). The bandwidth of the valves used in the experiments was

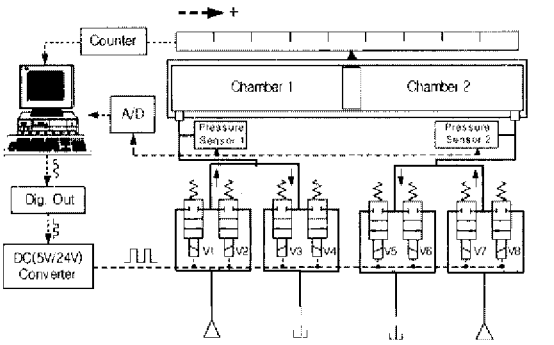

Fig. 1 Schematic diagram of pneumatic control system

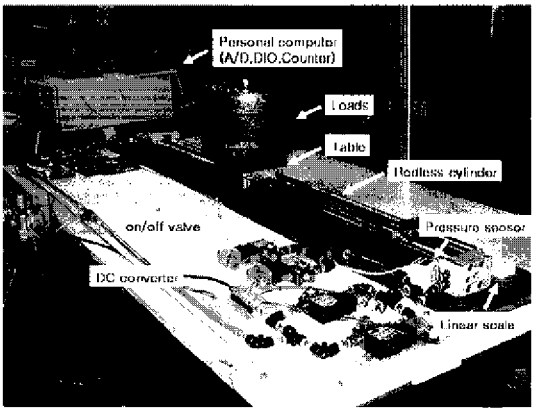

Fig. 2 Photograph of experimental apparatus

250 Hz. The experiments were conducted under a pressure of 0.5 MPa and all control software was coded in C. A photograph of the experimental apparatus was shown in Fig. 2.

2.2 Characteristics of the on/off solenoid valve

When using on/off solenoid valves to control the position of a pneumatic cylinder, it is necessary to understand the characteristics of the on/off solenoid valve. This includes the dead-time and the rise time of valve, the maximum current, etc. Figure 3 shows the current of the solenoid valve when the ON signal was applied to the on/off solenoid valve for 100 ms. The current was measured from the voltage drop across the resistance, which is serially connected to the solenoid valve.

In the zoom graph of Fig. 3, the valve started to move after t_a and the valve was fully opened after t_b. This means that the valve started to move when the duration of the ON pulse to the valve was longer than 4 ms.

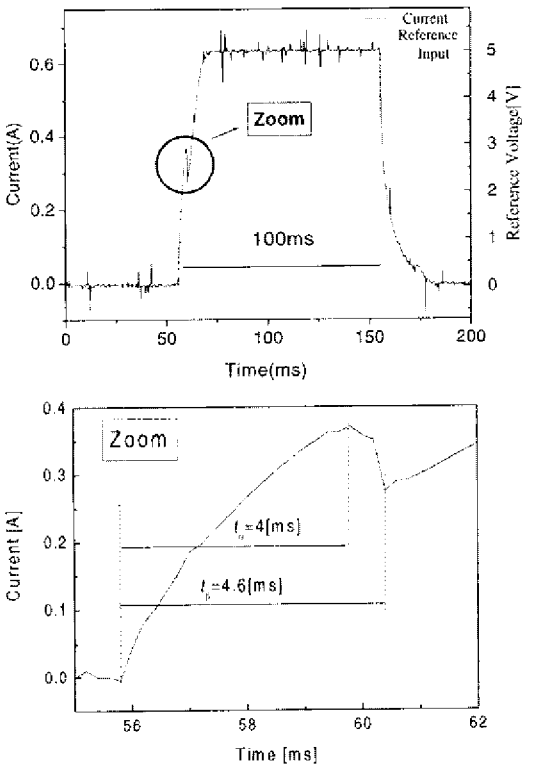

Fig. 3 Measurement of valve opening time

2.3 Modified PWM algorithm

When using on/off solenoid valves to control the position of the cylinder, the control input u must be converted into the pulse width modulation on/off signal in each solenoid valve. Previous studies have used 1) a conventional PWM scheme (Noritsugu, 1986, 1987; Muto, 1993), where the valve opening time was proportional to the magnitude of the control input and 2) a modified PWM scheme (Shih, 1996, 1997), where the dead time of valve and other nonlinear terms were considered. In modified PWM scheme, the dead-time of on/off solenoid valves is important in the design of our PWM algorithm because the valve failed to move if the duration time of ON signal to the solenoid valve was shorter than the dead-time of the valve. To overcome this problem, we applied a modified PWM algorithm, where the minimum pulse width time was added to the output of the conventional PWM even if the control input was very small. However, the control input became zero within any allowable position error in order to prevent the oscillation of an actuator or a valve near the reference position. The limit of position error is expressed by ε in equation 1.

$$
\begin{aligned}
U_{MPWM}(t) &= \begin{cases} sign(U(k)) \cdot U_0 & (k-1)T \le t \le (k-1)T + t_b(k) \\ 0 & (k-1)T + t_b(k) \le t < kT \end{cases} \\
t_b(k) &= \begin{cases} t_s(k) & , 0 \le t_s(k) < T \\ T & , t_s(k) \ge T \end{cases} \\
t_s(k) &= \begin{cases} 0 & , |y_{ref} - y| \le \varepsilon \\ t_{s1} & , |y_{ref} - y| > \varepsilon \end{cases} \\
t_{s1}(k) &= \begin{cases} \dfrac{|U(k)|}{U_{max}} T + t_{DZ} & , 0 < |U(k)| \le U_{max} \cdot (1 - t_{DZ}/T) \\ T & , |U(k)| > U_{max} \cdot (1 - t_{DZ}/T) \end{cases}
\end{aligned}
\tag{1}
$$

Our proposed modified PWM (MPWM) valve pulsing method is shown in equation 1 and one example of the MPWM output with respect to the continuous control signal is shown in Fig. 4 where the MPWM period is 10 ms. Particularly, the same size of paired on/off solenoid valves (V1 and V2, V3 and V4, V5 and V6, V7 and V8 in Fig. 1) were used in order to improve the control

performance of this pneumatic system. Figure 5 shows a comparison of system responses according to 4 types of valve combinations.

From Fig. 5, it is understood that system responses of this pneumatic system depended more on the on/off valve in the exhaust part (V3 and V4, V7 and V8 in Fig. 1) rather than the on/off valve in the supply part (V1 and V2, V5 and V6 in Fig. 1).

If the control input is positive and greater than UBmaxB(Saturated Control Input), V1, V2 valves are used as intake valves and V5, V6 valves are used as exhaust valves to improve the rising time. If the control input is positive and less than U_{max}, only V1 and V5 valves are used as intake and exhaust valves, respectively.

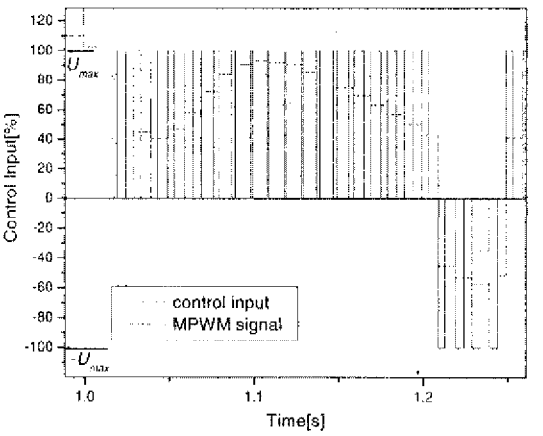

Fig. 4 Example of the MPWM signal

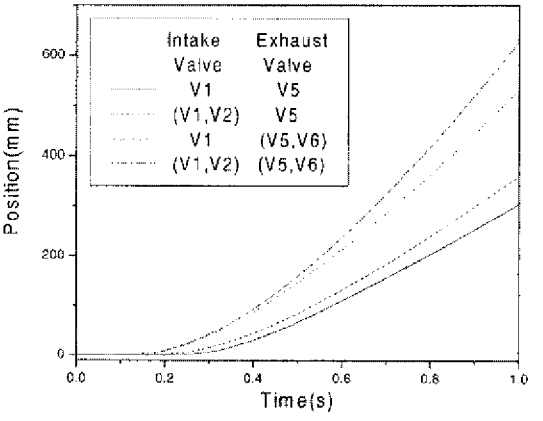

Fig. 5 Comparison of system response according to valve combination

Conversely, If the control input is negative and less than $-U_{max}$, V7, V8 valves are used as intake valves and V3, V4 valves are used as exhaust valves. If the control input is negative and greater than $-U_{max}$, only V7 and V3 valves are used as intake and exhaust valves, respectively.

3. Intelligent Switching Control Algorithm of the Pneumatic System

3.1 The overall control system

In order to appropriately adjust the control parameters according to external loads, load conditions must be recognized using dynamic information of the pneumatic system in an on-line manner. Here we applied the LVQNN as a means of supervisor, which classifies 4 typical external loads (0, 10, 20, 30 Kg). The overall control system with the LVQNN as supervisor was shown in Fig. 6. To control the pneumatic system, a 3-state feedback control algorithm was applied in this paper, where the position, velocity and acceleration of the rodless cylinder were used. It is reported that a 3-state feedback control method was effective in the pneumatic control system (Weston, 1984 ; Klein, 1993). The controller output at sampling sequence k becomes

$$u(k)=k_p(y_d(k)-y(k))-k_v v(k)-k_a a(k) \quad (2)$$

where $u(k)$, $y(k)$, $v(k)$, $a(k)$, $y_d(k)$, k_p, k_v and k_a represent control input, position, velocity and acceleration of the rodless cylinder, reference position, proportional gain, velocity gain and acceleration gain, respectively. The control input u is calculated from position, velocity and acceleration of the rodless cylinder and is converted

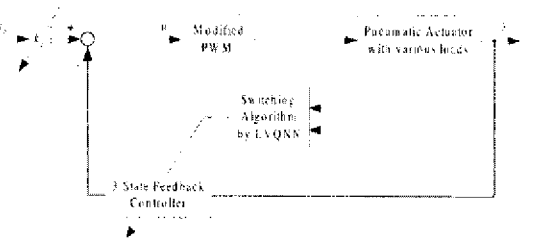

Fig. 6 Structure of newly-proposed control algorithm

into a pulse width modulation signal to operate the on/off solenoid valves.

3.2 Classification of load conditions by the LVQNN

The LVQNN was utilized here for classifying input patterns with inherent class intersections. The core of the LVQNN is based on the nearest-neighbor method by calculating the Euclidean distance. During training stage, the values of weights are adjusted according to the patterns of input samples in order to match with desired classes. The distance of an input vector to the weight vector of each node in Competitive layer is computed.

The node of a particular class which has the smallest distance is declared to be the winner. The weights will be moved closer to the class if it is the expected winning class, otherwise they will be moved away. After the training process is finished, the LVQNN is then ready for classifying unknown input vectors. During the evaluating stage, the distance of an unknown input vector to each of all classes' reference vectors is calculated again. After computing the distance to this input vector and each reference vector, the node which has the closest distance to the input vector is declared to be the winner. Then the unknown input vector will be assigned to the class which the reference vector belongs to.

3.2.1 Structure of the neural classifier

Figure 7 shows the architecture of the LVQNN, where P, y, W_1, W_2, R, S_1, S_2 and T denote input vector, output vector, weight of competitive layer, weight of linear layer, the number of neurons in the input layer, competitive layer, linear and target layer, respectively. The LVQNN is a supervised learning algorithm and is composed of 2 layers. The first is the competitive layer which functions the learning of the classification of the input vector. The second is the linear layer which classifies the competitive layer according to a designer's intention.

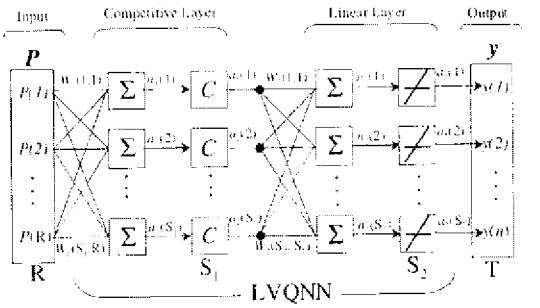

Fig. 7 Structure of the LVQNN

For the generation of training data, the valves were fully opened in order to move the rodless cylinder in a forward direction. This is explained in the next section.

For each input vector $P(j)$, a winner neuron $W_1(i, j)$ is chosen to adjust its weight vector: (Wang, 1996)

$$\|P(j) - W_1(i, j)\| \leq \|P(j) - W_1(k, j)\|, \ \forall k \neq i \quad (3)$$

The weight vector $W_1(i, j)$ is updated to the next step by the following Kohonen (1987) learning rule.

$$\Delta W_1(i, j) = \lambda \cdot a_1(i) \cdot (p(j) - W_1(i, j)) \quad (4)$$

where λ is the learning ratio and $a_1(i)$ is the output of competitive layer.

The output of competitive layer $a_1(i)$ becomes 1 if the input pattern is classified correctly and 0 if the input pattern is classified incorrectly.

3.2.2 Data generation for the training of the LVQNN

In this section, the training data for the LVQNN is explained in detail. The input and output data of LVQNN are shown in Fig. 8. The input data for the LVQNN is the velocity of the rodless cylinder, and the output of the LVQNN is a class among 4 discrete classifications, where 4 cases were classified according to the external load. For example, class 3 indicates that the range of the external load was approximately between 15 kg and 25 kg, as shown in Table 1. To obtain training data for the LVQNN, a series of experiments were conducted under 12 different load conditions, as shown in Table 1. In experiments for the generation of training data, the initial position of rodless cylinder was set to 80 mm and the four valves (V1, V2, V5 and V6 in Fig. 1)

Table 1 Classification of external load

No.	Class 1	Class 2	Class 3	Class 4
1	**0 kg**	8 kg	18 kg	28 kg
2	2 kg	**10 kg**	**20 kg**	**30 kg**
3	4 kg	12 kg	22 kg	32 kg

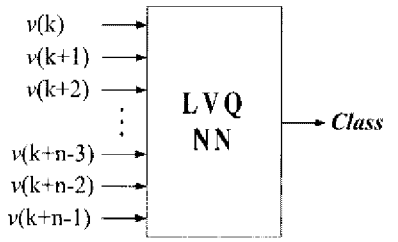

Fig. 8 Training data for the LVQNN

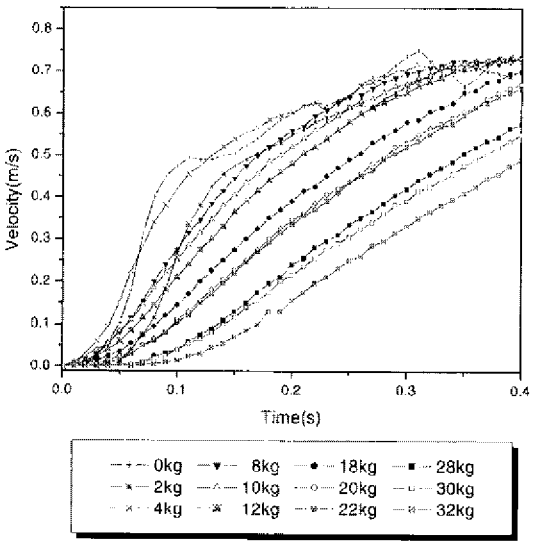

Fig. 9 Experimental results for training data generation

were fully opened for 0.4 s in order to make the rodless cylinder move in a forward direction at full speed.

Therefore, a total 12 cases of experiments were carried out to prepare for the training data of the LVQNN, as shown in Fig. 9. As the load increased, the system response became slower and had more of a time delay. From Fig. 9, the external load may be classified by using the LVQNN. In the training stage of the LVQNN, the numbers of input vectors were adjusted from 27 to 32 and the number of neurons in the competitive layer was adjusted from 20 to 40 in 10 steps in order to obtain the optimal parameters of the LVQNN. From Table 2, it is understood that the optimal number of input vectors and the number of neurons of the competitive layer were 30 and 40 respectively.

Table 2 Training success rate of the LVQNN

NCL \ NIV	27	28	29	**30**	31	32
20	94.1%	95.5%	97.2%	98.5%	97.5%	98.1%
30	98.8%	98.7%	99.3%	97.7%	99.1%	100%
40	98.8%	98.1%	99.3%	**100%**	100%	100%

Leaning rate : 0.04
Training Epoch : 10000
NIV : Number of Input Vector
NCL : Number of Competitive Layer

3.3 Proposition of the smooth switching algorithm

If the load condition is different from its load condition used in the training, the output of the LVQNN may not belong to the predefined class, but to mixed classes with different ratios in each class (i.e. if the external load is 25 kg, it may belong to 3 or 4 class). Therefore, the following switching algorithm was proposed to apply to abrupt changes of external loads as follows.

$$\text{class}(k) = \lambda \times \text{class}(k-1) + (1-\lambda) \times \text{class}(k) \quad (5)$$

where k is discrete sequence, λ is forgetting factor and class(k) is the output of the LVQNN at k time sequence. The selection of λ is dependent on one cycle time of MPWM signal and the convergence rate of each control parameter. In our experiment, one cycle time of MPWM signal and convergence time of classification was set to be 10 [ms] and 0.1 [s], respectively. The initial value of class was set to be 1 and tti was selected to be 0.53 in order to reach the target class within 1% error with respect to the true class within 0.1 [ms]. By this setting of λ, the calculated class becomes 3.9901(within 1% error) after 0.1 [ms] if the estimated classes all belongs to 4.

The optimal parameters of the 3-loop controller and the MPWM were obtained by a trial-and-error method through experiments, which

Table 3 Optimal parameters of 3-loop controller and MPWM

Class No.	K_v	U_{max}	K_p	K_a
1	0.07	60	1.5	0.001
2	0.12	100		
3	0.166	150		
4	0.195	200		

are shown in Table 3. From Table 3, it may be understood that velocity feedback gain (K_v) and saturated control input (U_{max}) increased according to an increase of external loads and had to be automatically switched according to the external load.

The following equations are the updating laws of velocity feedback gain (K_v) and saturated control input (U_{max}).

$$K_v(k) = K_v(p) \times (q - \text{class}(k)) + K_v(q) \times (\text{class}(k) - p) \quad (6)$$

$$U_{max}(k) = U_{max}(p) \times (q - \text{class}(k)) + U_{max}(q) \times (\text{class}(k) - \text{p}) \quad (7)$$

$$p = \text{floor}(\text{class}(k)),\ q = \text{ceil}(\text{class}(k)) \quad (8)$$

where k is discrete sequence, class(k) is the output of the LVQNN at k time sequence, function floor($\cdot$) rounds to the nearest integer greater than or equal to the input value and function ceil($\cdot$) rounds to the nearest integer greater than or equal to the input value. For example, floor(1.7) equals 1 and ceil(1.7) equals 2.

4. Experiments

Experiments without external loads are shown in Fig. 10. The reference position of the rodless cylinder is set to be 600 mm, the experiment time for 3 s and the proportional, velocity and acceleration gains (k_p, k_v, k_a) of the 3-state feedback controller were set to be 1.5, 0.065 and 0.0001, respectively. These control parameters were based on the following design specifications.

- Maximum overshoot : within 0.3[%]
- Settling Time : less than 1.5[s]

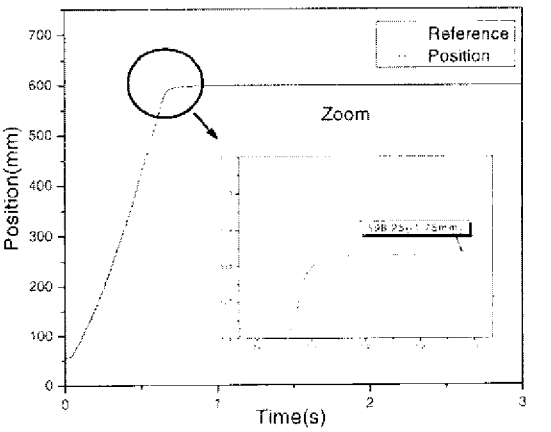

(a) In the case of conventional PWM

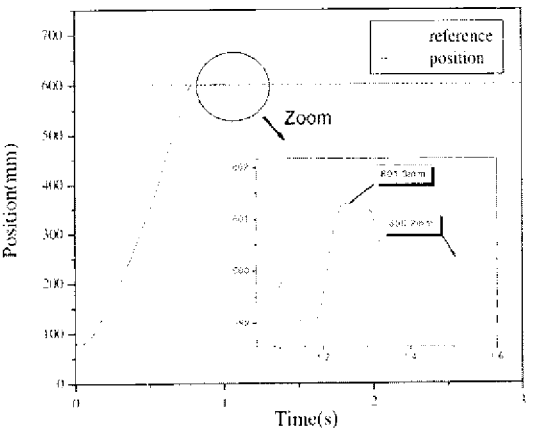

(b) In the case of proposed MPWM

Fig. 10 Experimental results of rodless cylinder

The steady state error was about 1.75 mm in the case of the conventional PWM algorithm and about 0.2 mm in the case of our proposed MPWM algorithm as seen in Fig. 10. From the experimental results, it was verified that the proposed MPWM method was very effective in the accurate position control of the pneumatic system. Figure 11 shows the experimental results of position control with different external loads (10 kg, 20 kg and 30 kg), where the control gains were the same as that of the unloading condition. From Fig. 11, it may be understood that the system response became more oscillatory according to an increase of external load and this suggested that the control parameters must be adjusted according to the variations of the external load. Next, experiments were carried out to verify

the effectiveness of our proposed MPWM and switching algorithm by the LVQNN. These experimental results are shown in Figs. 12 and 13, which correspond to 20 Kg and 30 Kg in the external load, respectively. In the figure, position, velocity and acceleration of the rodless cylinder and control input, the output of the LVQNN and the MPWM pulsing signal are shown respectively in each figure. The output of the LVQNN started to take effect only after the magnitude of velocity of rodless cylinder was greater than 0.5 [m/s]. From these experimental results, it was verified that the external load condition was correctly recognized by class number 3 and 4, respectively, and that the accurate position control was also realized with a steady state error of 0.2 [mm].

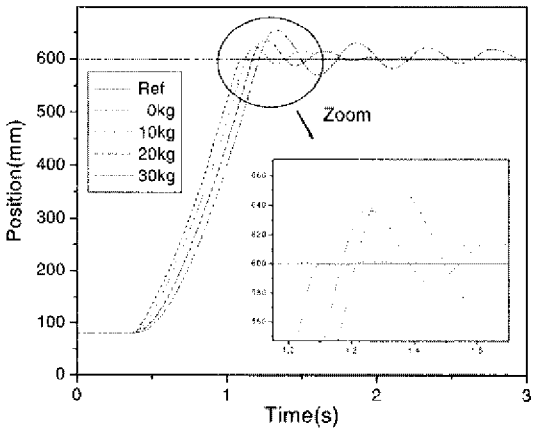

Fig. 11 Experimental results of rodless cylinder without switching control with respect to four different loads

Experimental results with a 25 kg load condition are shown in Fig. 14. This load condition corresponded to the class 3 and 4. The class number calculated from the output of the LVQNN was 3.45, which proved that the external load was between 20 and 30 kg. The velocity feedback gain (K_v) and saturated control input ($U_{\max}$) were updated using the updating laws of Eqs. (5) and (6).

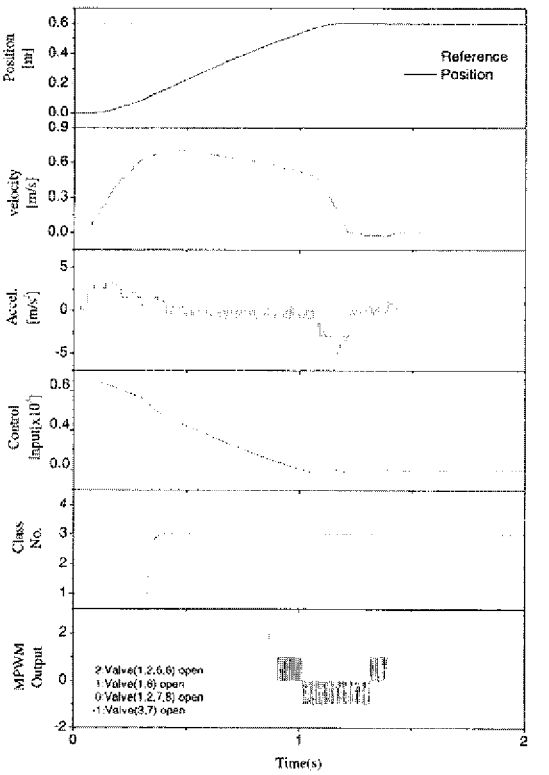

Fig. 12 Experimental results when external load is 20 kg

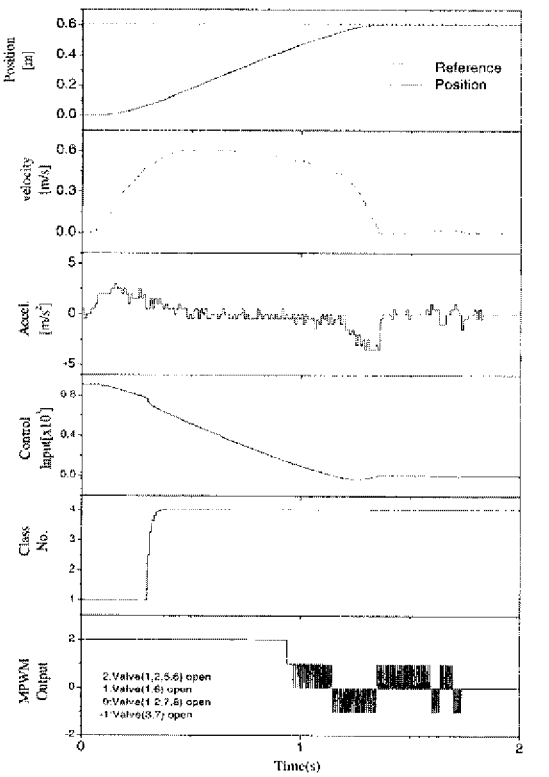

Fig. 13 Experimental results when external load is 30 kg

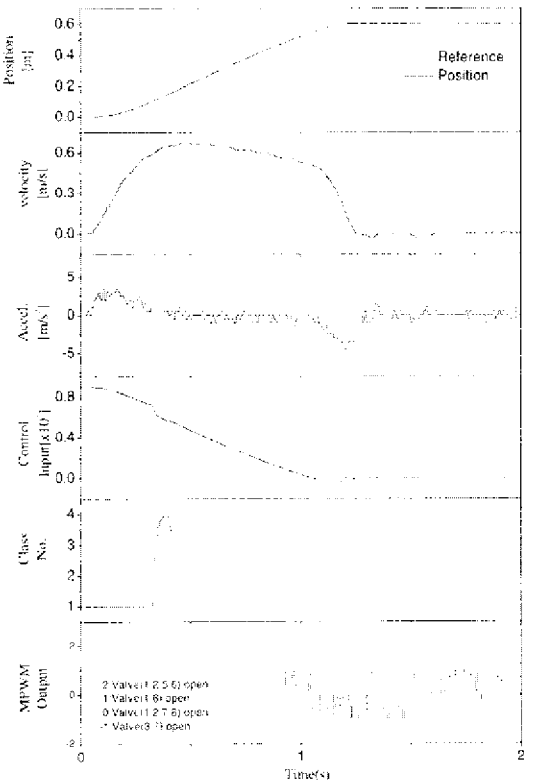

Fig. 14 Experimental results when external load is 25 kg

In Fig. 15, experiments were conducted to compare system responses with respect to 4 different weight conditions (0, 10, 20 and 30 kg) with and without the proposed switching algorithm by the LVQNN. From these experimental results, it was found that the system response became oscillatory according to an increase of the external load. On the contrary, the system response was almost the same and the steady-state error was within 0.4 mm in any case when using our proposed switching algorithm by the LVQNN.

In Fig. 16, experiments were conducted to investigate the performance of our proposed control system with respect to abrupt changes of external load. The external load was abruptly changed from 20, 0 to 30 Kg and the experiment was executed for 5 seconds in each load condition. From the results of class classification (2nd row from bottom in Fig. 16), it was verified that our proposed switching algorithm by the LVQNN was very effective in the classification

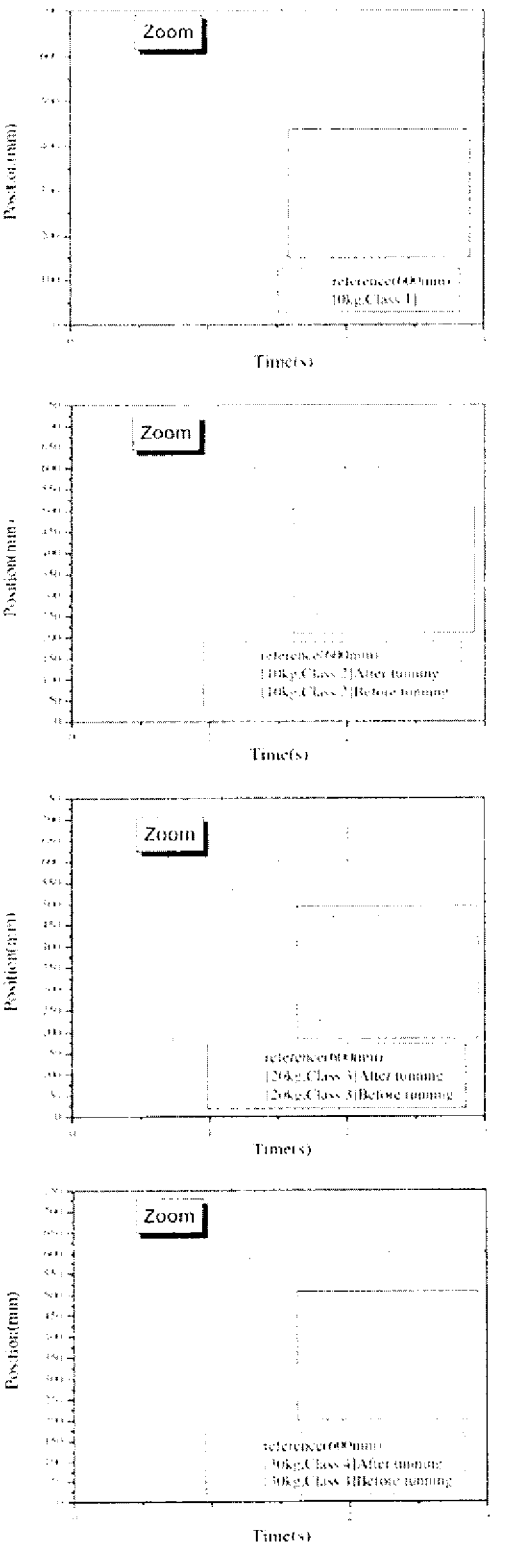

Fig. 15 Comparison of experimental results with and without the LVQNN

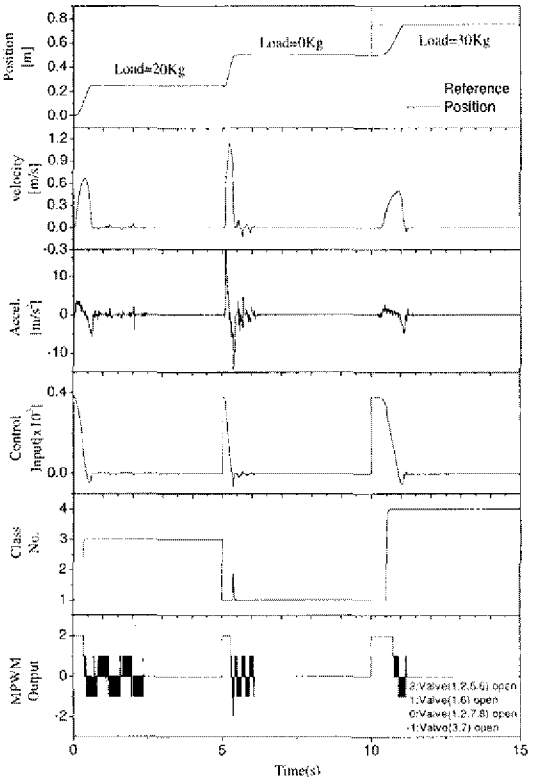

Fig. 16 Experimental results when external load changes step by step

of abrupt changes of external load and that the parameters of the controller were automatically adjusted by using a smooth switching algorithm and that the control performance of transient responses was greatly increased with respect to abrupt changes of external load.

One of the application fields of this research is the loading/unloading task and a point to point control is important in such a task. This proposed algorithm can only work with step inputs because LVQNN was trained by the experimental data of step responses. Therefore LVQNN cannot recognize or recognize poorly the external load conditions in the case of sinusoidal input.

5. Conclusion

The first contribution of this paper was to develop a fast, accurate, inexpensive and external load independent pneumatic servo system using on/off valves. The position control was successfully implemented using on/off solenoid valves instead of expensive servo valves. The valves were pulsed using a modified PWM algorithm, which compensated for the dead-time of on/off valves. This was verified by experiments of position control in which steady state errors were reduced to within 0.2 mm.

The second contribution of this paper was to apply the learning vector quantization neural network (LVQNN) as a supervisor of switching controllers in pneumatic servo systems with an on/off valve, where the LVQNN functions to classify the condition of the external load and selects suitable gains of controller for each external load condition.

From the experiments of position control of pneumatic cylinder, it was verified that the proposed MPWM and smooth switching algorithm were very effective to overcome the deterioration of control performance of transient responses due to 4 different external loads.

Acknowledgment

This work was partly supported by the Korea Science and Engineering Foundation (KOSEF) through the Research Center for Machine Parts and Materials Processing (ReMM) at University of Ulsan.

References

Anderson, B. W., 1967, "Analysis and Design of Pneumatic Systems," *John Wiley and Sons*, New York.

Ahn, K. K. and TU, D. C. T., 2004, "Improvement of the Control Performance of Pneumatic Artificial Muscle Manipulators Using an Intelligent Switching Control Method," *KSME Int. J.*, Vol. 18, No. 8, pp. 1388~1400.

Kawamura, S., Miyata, K., Hanafusa , H. and Isida , K., 1989, "PI Type Hierarchical Feedback Control Scheme for Pneumatic Robots," *Proc. IEEE Int. Conf. Robotics and Automation*, 3, pp. 1853~1858.

Klein, A.. 1993, "Einsatz der Fuzzy-Logik zur Adaption der Positionsregelung Fluidtechnischer

Zylinderantriebe," Dissertation, RWTH Aachen

Kohonen, T, 1987, "Self-Organization and Associative Memory," Springer-Verlag, Berlin

Marchant, J A, Street, M J, Gurney, P and Benson, J A, 1989, "Design and Testing of a Servo Controller for Pneumatic Cylinders," *Proc Inst. Mech. Eng. E*, 203, pp 21~27

Mishra, J K and Radke, M G, 1994, "Reduced Order Sliding Mode Control for Pneumatic Actuator," *IEEE Trans on Control System Technology*, 2, pp 271~276

Muto, T, Kato, H, Yamada, H and Suematsu, Y, 1993, "Digital Control of an HST System with Load Cylinder Operated by Differential Pulse width Modulation," Proc of the 2nd JHPS International Symposium on Fluid Power, pp 321~326

Noritsugu, T, 1986, "Development of PWM Mode Electro-Pneumatic Servo Mechanism, Part I Speed Control of a Pneumatic Cylinder," *Journal of Fluid Control*, 17(1), pp 65~80

Noritsugu, T, 1987, "Development of PWM Mode Electro-Pneumatic Servo Mechanism, Part II Position Control of a Pneumatic Cylinder," *Journal of Fluid Control*, 17(2), pp 7~28

Noritsugu, T and Takaiwa, M, 1995, "Robust Position Control of Pneumatic Servo System with Pressure Control Loop," *Proc. IEEE int Conf. Robotics and Automation*, 3, pp. 2613~2618

Shih, M C and Hwang, C G, 1996, "Fuzzy PWM Position Control of a Pneumatic Robot Cylinder Using High Speed Solenoid Valves," *The Fourth JHPS International Conference on Fluid Power*, Yokohama, Japan

Shih, M C and Ma, M A, 1997, "Pneumatic Rodless Cylinder Position Control by Neuro Fuzzy Modified Differential PWM Control Method," *The Fifth Triennial Int Symp. on Fluid Control, Measurement and Visualization*, Hayama, Japan, pp 255~260

Tang, J and Walker, G, "Variable Structure Control of a Pneumatic Actuator," *Trans. of ASME, Journal of DSMC*, 117, pp 88~92

Wang, D D and Jinwu Xu, 1996, "Fault Detection Based on Evolving LVQ Neural Networks," *IEEE Int Conf. on Systems, Man, and Cybernetics*, pp 255~260

Weston, R H, Moore, P R and Thatcher, T W, 1984, "Computer Controlled Pneumatic Servo Drives," *Proc. Inst. Mech. Engrs*, 198 B (14), pp 225~231